

H₂-Binding by Neutral and Multiply Charged Titaniums: Hydrogen Storage Capacity of Titanium Mono- and Dications

Han Myoung Lee, Dong Young Kim, Chaeho Pak, N. Jiten Singh, and Kwang S. Kim*

Center for Superfunctional Materials, Department of Chemistry, Pohang University of Science and Technology, San 31, Hyojadong, Namgu, 790-784 Pohang, South Korea

ABSTRACT: Given that transition metal–hydrogen systems have been studied as a predecessor for hydrogen storage materials, we have investigated the neutral and multiply charged titanium–H₂ systems (Ti–H₂, Ti⁺–H₂, Ti²⁺–H₂, Ti³⁺–H₂, and Ti⁴⁺–H₂) using density functional theory (DFT) and high-level ab initio calculations, including coupled cluster theory with single, double, and perturbatively triple excitations [CCSD(T)]. These systems show different types of hydrogenation depending on their charged state. The neutral Ti–H₂ system shows dihydride structure with covalent interaction where the Ti–H distance is 1.76 Å, while H₂ is dissociated into two neighboring hydride ions by withdrawing electrons from Ti. The charged Ti⁺–H₂, Ti²⁺–H₂, and Ti³⁺–H₂ systems show dihydrogen structures with noncovalent interaction, where the Ti⁺–H, Ti²⁺–H, and Ti³⁺–H distances are 2.00, 2.14, and 2.12 Å, respectively. The main binding energies in these systems arise from the hydrogen polarizability driven interaction by the positive charge of Tiⁿ⁺ ($n = 1–3$). Among Tiⁿ⁺–H₂ ($n = 1–3$) the Ti⁺–H₂ has the shortest distance against our common expectation, while Ti²⁺–H₂ has the longest distance. The Ti⁺–H₂ distance is the shortest because of the d–σ* molecular orbital (MO) interaction which is not present in Ti²⁺–H₂ and Ti³⁺–H₂. The Ti⁴⁺ ion does not bind H₂. In this regard, we have investigated the maximal hydrogen binding capacity by Ti complexes. The coordination of titanium mono- and dications complexed with dihydrogen (H₂) [Ti⁺(H₂)_n and Ti²⁺(H₂)_m] is studied along with their structures, binding energies, electronic properties, and spectra. The titanium monocations of the quartet ground state have up to the hexacoordination, while titanium dications of the triplet ground state have up to the octacoordination at very low temperatures. At room temperature, the monocations favor penta- to hexacoordination, while the dications favor hexacoordination. This information would be useful for the design of hydrogen storage devices of Ti complexes, such as Ti-decorated/dispersed polymer–graphene hybrid materials.

I. INTRODUCTION

Development of the safe, reliable, compact, and cost-effective hydrogen storage medium is a technically challenging issue facing the “hydrogen economy”.¹ Two major techniques for hydrogen storage is to store hydrogen in the atomic form of hydrides and in the molecular form in sorbents. Some of metal hydrides, complex hydrides,² simple hydrogen-containing chemicals,³ and mixtures of these⁴ have shown promising results as hydrogen capacious materials at ambient conditions. They not only meet the ultimate goal of the system capacity with 7.5 wt % H₂ set by the U.S. Department of Energy (DOE)⁵ but also release hydrogen at ~363 K, which is the operating temperature of proton exchange membrane (PEM) fuel cells. However, no materials explored to date exhibit practical utility. On the other hand, hydrogen sorbents, such as carbon-based nanostructures and metal/covalent organic frameworks, show fast adsorption and desorption kinetics.⁶ However, because they are conventionally based on physisorption by the weak van der Waals interactions, they store hydrogen at high pressures and very low temperatures. While many researchers have been trying to strengthen the interaction between the sorbents and hydrogen, the use of the Kubas-typed orbital interaction (metal–σ interaction)⁷ would be an ideal strategy to make new generation of hydrogen sorbents.

Ti-decorated organometallic systems are suggested as good hydrogen storage nanomaterials through theoretical study.⁸ Transition-metal–π complexes (especially titanium complexes)⁹ and titanium metal–organic frameworks are also suggested as a

H₂ storage material.¹⁰ Porphyrins incorporated with the first-row transition metals were reported for their binding energies with a hydrogen molecule,¹¹ where the binding energy by Ti was the largest. The adsorption of H₂ on a series of 3d transition-metal (TM)-doped organosilica complexes was investigated by using theoretical methods.¹² The modified benzene–silica model with Sc, Ti, V, Cr, and Mn transition-metal atoms could adsorb H₂ into the dihydride or dihydrogen configuration forms. The structural, energetic, and electronic properties of small hydrogenated titanium clusters were studied.¹³ Their electronic structures were dealt with as a function of the number of adsorbed hydrogen atoms, which is an important issue in nanocatalysis and hydrogen storage. Given that the information of the structures and coordination of molecular clusters has been utilized to design novel functional materials,¹⁴ we have been interested in investigating the structure and coordination of neutral and multiply charged hydrogenated transition metals for possible design of organometallic compounds useful for hydrogen storage materials.

Transition metals have long been investigated for their catalytic properties in the hydrogenation reactions. Thus, their dihydrogen–metal complexes, where H₂ molecules were bound as intact molecular ligands, were investigated. The cation–(H₂)_n clusters with various first-row transition metal ions, such as Sc,¹⁵ Ti,¹⁶ V,¹⁷ Cr,¹⁸ Mn,¹⁹ Fe,²⁰ Co,²¹ Cu,²² and Zn,¹⁹ were reported.

Received: December 23, 2010

Published: March 16, 2011

Table 1. Binding Energies, Selected Geometrical Parameters, NBO Charges of Ti, and Selected Frequencies of $\text{Ti}^{0/1+/2+/3+}-\text{H}_2$ Complexes^a

method	$-\Delta E$	$-\Delta E_0$	$-\Delta H_r$	$-\Delta G_r$	$d_{\text{H}-\text{H}}$	$d_{\text{Ti}-\text{H}}$	$q(\text{Ti})$	ν_{H_2}	$\nu_{\text{Ti}-\text{H}_2}^{\text{asym}}$	$\nu_{\text{Ti}-\text{H}_2}^{\text{sym}}$
$\text{Ti}-\text{H}_2$										
B3LYP/W*QZ	16.47	17.40	18.47	13.53	3.08	1.76	—	(573) ^b	1593	1582
MP2/W*QZ	10.61	11.80	12.83	7.89	3.18	1.75	1.222	(458) ^b	1568	1559
CCSD(T)/W*QZ	11.82	13.03	14.04	9.15	3.19	1.76	—	(436) ^b	1572	1543
Ti^+-H_2										
B3LYP/W*QZ	11.60	9.90	11.00	5.78	0.77	2.03	—	3839	1036	712
MP2/W*QZ	11.75	9.89	10.99	5.76	0.76	2.00	1.031	3969	1013	683
CCSD(T)/W*QZ	9.53	7.70	8.80	3.55	0.77	2.00	—	3904	1057	718
$\text{Ti}^{2+}-\text{H}_2$										
B3LYP/W*QZ	20.50	19.03	20.09	15.00	0.78	2.17	—	3958	784	686
MP2/W*QZ	17.88	16.31	17.37	12.28	0.76	2.16	1.978	4024	770	675
CCSD(T)/W*QZ	19.20	17.57	18.63	13.51	0.77	2.14	—	4037	783	720
$\text{Ti}^{3+}-\text{H}_2$										
B3LYP/W*QZ	—	—	—	—	—	—	—	—	—	—
MP2/W*QZ	53.26	52.79	53.79	48.77	0.83	2.05	2.827	3372	947	455
CCSD(T)/W*QZ	56.94	57.37	58.51	53.35	0.84	2.12	—	3226	903	159

^a ΔE and ΔE_0 are the binding energies (kcal/mol) without/with zero-point energy correction; ΔH_r and ΔG_r are the enthalpy and free-energy changes (kcal/mol) at room temperature and 1 atm; $d_{\text{H}-\text{H}}$ is H—H distance (Å); and $d_{\text{Ti}-\text{H}}$ is the distance (Å) between a Ti ion and a H atom of H_2 . The H—H distance of pure H_2 molecule is 0.742, 0.736, and 0.742 Å at the B3LYP, MP2, and CCSD(T) levels, where the aug-cc-pVQZ set was used for hydrogen and the [9s7p5d3fg] contracted basis set (W*) was used for Ti; and $q(\text{Ti})$ is the natural bond orbital charge (au) of the Ti ion at the MP2 level. The NBO charges are given at the MP2 level; ν_{H_2} is the scaled stretching frequency (cm^{-1}) of the H_2 molecule; and $\nu_{\text{Ti}-\text{H}_2}^{\text{asym}}$ and $\nu_{\text{Ti}-\text{H}_2}^{\text{sym}}$ are scaled asymmetric and symmetric Ti— H_2 stretching frequencies (cm^{-1}). The experimental H—H stretching frequency of the H_2 molecule is 4401 cm^{-1} (ref 28). ^b Bending frequencies of Ti— H_2 .

Their objectives were to obtain the structures and binding energies of metal ion—(H_2)_n complexes and to understand the σ -bond activation processes for the H—H bond and for the C—H bonds in hydrocarbons. Since the binding of Ti^+ with H_2 was predicted to be the largest among first transition metals,¹⁶ we here investigate dihydrogen—titanium complexes. The charged state of titanium atom plays an important role in complexation.²³ We report the structures, binding energies, and electronic properties of titanium mono- and dications binding dihydrogen (H_2) molecules [$\text{Ti}^+(\text{H}_2)_{n=1-7}$ and $\text{Ti}^{2+}(\text{H}_2)_{m=1-9}$] using density functional theory (DFT) and high-level ab initio theory.

II. CALCULATION METHODS

For all Möller–Plesset second-order perturbation (MP2) and coupled cluster theory with single, double, and perturbatively triple excitations [CCSD(T)] calculations presented here, all electrons were correlated, the unrestricted open shell approach was employed, and the basis set superposition error (BSSE) correction was made. The calculations were carried out by using the Gaussian 03 suite of programs.²⁴ Molecular structures and molecular orbital contour maps were drawn using the Posmol package.²⁵

For $\text{Ti}^{n+}-\text{H}_2$ ($n = 0-4$), we have used DFT with Becke's three-parameters for exchange and Lee–Yang–Parr correlation functional (B3LYP) in the investigation of neutral and cationic hydrogen—titanium clusters. The aug-cc-pVQZ set is employed for hydrogen. By extending the Ti basis set of the Wachters+f set [8s6p4df] (close to the ccpVTZ and aug-cc-pVDZ levels, which will be denoted as W),²⁶ we have made the optimized [9s7p5d3fg]

contracted functions (similar to ccpVQZ and aug-ccpVTZ levels, which will be denoted as W*). All the “d” and “f” orbitals are the spherical harmonic basis functions (5d and 7f). The combined basis set of W and aug-cc-pVTZ will be simply denoted as WTZ for simplicity, and that of W* and aug-cc-pVQZ will be denoted as W*QZ. Since B3LYP results are not reliable in the present system, the important structures were calculated at the MP2 level using the same basis sets. To obtain more accurate results, the CCSD(T)/W*QZ calculations were employed. At the CCSD(T)/W* level the initial $\langle S^2 \rangle$ values of $\text{Ti}^{0/1+/2+/3+}$ are 2.010, 3.753, 2.003, and 0.752, and the T1 diagnostic values of $\text{Ti}^{0/1+/2+/3+/4+}$ are 0.0145, 0.0049, 0.0023, 0.0015, and 0.0008, respectively. The spin multiplicities of $\text{Ti}^{0/+ /2+/3+/4+}$ are triplet, quartet, triplet, doublet, and singlet, respectively. The CCSD(T)/W* ionization energies for $\text{Ti}^{+/2+/3+/4+}$ are 151.1, 309.5, 632.4, and 999.3 kcal/mol, in agreement with the experimental values (157.3, 313.1, 634.1, and 997.8 kcal/mol).²⁷ At each calculation level the structures were fully optimized along with vibrational frequencies. The frequencies were employed to obtain the zero-point energies (ZPE) and the enthalpy/free-energy changes ($\Delta H_r/\Delta G_r$) at room temperature and 1 atm. To investigate their stabilities, the binding energies of ΔE_e and ΔE_0 between Ti ions and H_2 were calculated without and with ZPE correction, respectively. The frequencies were scaled by scale factors (0.997 at the B3LYP/W*QZ, 0.975 at the MP2/W*QZ, and 1.000 at the CCSD(T)/W*QZ level) to match the experimental frequency (4401 cm^{-1})²⁸ of the H_2 molecule. Though the neutral Ti— H_2 complex forms a covalent bond between a neutral Ti atom and two hydrogen atoms, multicationic charged complexes show noncovalent interactions between a Ti ion and a

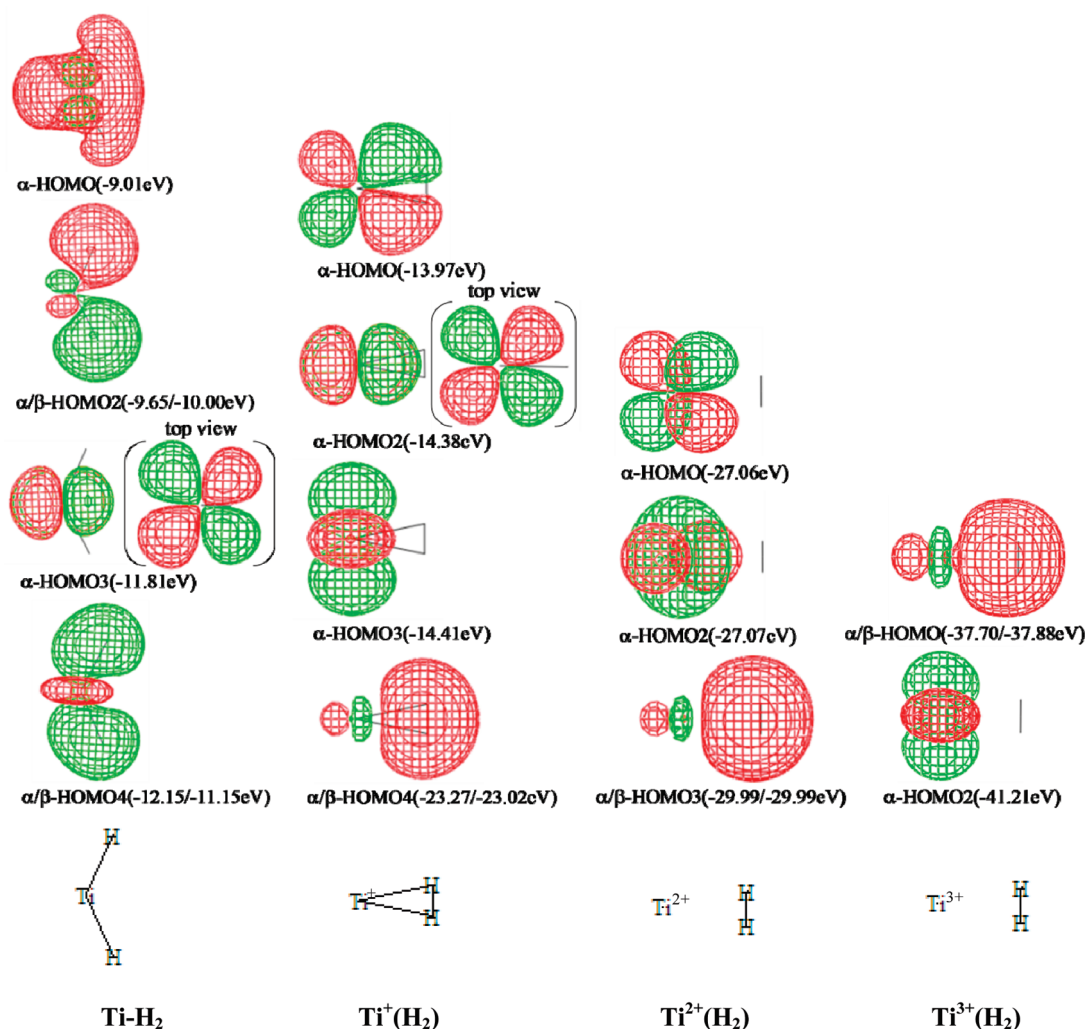


Figure 1. HOMOs of the Ti-H_2 , Ti^+-H_2 , $\text{Ti}^{2+}-\text{H}_2$, and $\text{Ti}^{3+}-\text{H}_2$ complexes (at the CCSD(T)/WTZ level). The orbital energies are in parentheses.

hydrogen molecule. The natural bond orbital (NBO) charges were obtained at the MP2/W*QZ level of theory.

We investigated various possible structures of $\text{Ti}^+(\text{H}_2)_{n=1-7}$ and $\text{Ti}^{2+}(\text{H}_2)_{m=1-9}$. The low-energy structures were initially investigated by B3LYP/WTZ and further calculated by the MP2/WTZ. The structures were fully optimized along with their vibrational frequency analysis. The CCSD(T)/WTZ calculations were performed on the MP2/WTZ optimized geometries. At the CCSD(T)/W level the initial $\langle S^2 \rangle$ values of Ti^+ and Ti^{2+} ions were 3.75 and 2.00, and their T1 diagnostic values were 0.0060 and 0.0040, respectively. At the CCSD(T)/W level the energy difference between Ti^+ and Ti^{2+} ions was estimated to be 306.9 kcal/mol, in agreement with the experimental value (313.1 kcal/mol).²⁷ The CCSD(T)/WTZ thermodynamic quantities (ΔE_0 at 0 K; ΔH_r and ΔG_r at room temperature and 1 atm) were estimated using the CCSD(T)/WTZ single point interaction energies (ΔE_e) and the MP2/WTZ ZPE and thermal energies. The NBO charges (q^{NBO}) were estimated through NBO population analysis at the MP2/WTZ level of theory. Their B3LYP/WTZ and MP2/WTZ frequencies were scaled by scale factors (0.966 and 0.975) to match the experimental frequency (4401 cm^{-1})²⁸ of the H_2 molecule.

III. RESULTS AND DISCUSSION

The binding energies, selected geometrical parameters, NBO charges of $\text{Ti} [q(\text{Ti})]$, and selected frequencies of $\text{Ti}^{0/1+/2+/3+}-\text{H}_2$ complexes, which were calculated at the levels of B3LYP, MP2, and CCSD(T) using the W*QZ basis set, are listed in Table 1. The $q(\text{Ti})$ values of the $\text{Ti}^{0/1+/2+/3+}-\text{H}_2$ complexes are 1.22/1.03/1.98/2.83 au. Figure 1 shows the frontier highest occupied molecular orbitals (HOMO) of Ti-H_2 , Ti^+-H_2 , $\text{Ti}^{2+}-\text{H}_2$, and $\text{Ti}^{3+}-\text{H}_2$ complexes at the CCSD(T) level with the WTZ basis set, for visual aid, because those with W*QZ are hard to be legible due to the diffuse nature of the orbitals.

The neutral Ti-H_2 complex shows the covalent-bonded Ti-dihydride structure. The spin multiplicity for the ground state of the Ti-H_2 complex is triplet. It has a bent shape like the water molecule (H_2O). The binding energy without/with ZPE correction ($-\Delta E_e/\Delta E_0$) is 16.47/17.40, 10.61/11.80, and 11.82/13.03 kcal/mol at the B3LYP/W*QZ, MP2/W*QZ, and CCSD(T)/W*QZ levels. As for the HOMO, the $\alpha\text{-HOMO}$ is composed of the hybridized orbital of 4s and 3d orbitals of Ti and the σ orbital of H_2 . A doubly occupied d orbital of Ti and the σ^* orbital of H_2 form the second $\alpha/\beta\text{-HOMO}$ ($\alpha/\beta\text{-HOMO2}$), which leads to the strong backdonation to the $\text{H}_2\sigma^*$ orbital,

inducing the bent structure. Thus, the NBO charge (q) of H atoms is negative and that of Ti atom is positive ($q_{\text{Ti}} = 1.22$ au, $q_{\text{H}} = -0.61$ au at the MP2/W*QZ level). The third α -HOMO (α -HOMO3) is a singly occupied nonbonding d orbital. The fourth α/β -HOMO (α/β -HOMO4) is a bonding orbital between an unoccupied d_{z^2} orbital and a doubly occupied $\text{H}_2\sigma$ orbital.

At the B3LYP/W*QZ level the complex has a relatively weak orbital interaction between an occupied d orbital and the unoccupied $\text{H}_2\sigma^*$ orbital, which leads to the very strong $d-\sigma^*$ backdonation as compared with the cases at the MP2/W*QZ and CCSD(T)/W*QZ levels. This backdonation is due to the third α/β -HOMO (α/β -HOMO3) at the B3LYP/W*QZ level, the second α/β -HOMO (α/β -HOMO2) at the CCSD(T)/W*QZ level, and the α/β -HOMO at the MP2/W*QZ level. Therefore, the B3LYP/W*QZ binding energy is larger than the MP2/W*QZ value. This effect results in slightly different bond angles: 122.3° at the B3LYP/W*QZ level, 129.7° at the CCSD(T)/W*QZ level, and 131.0° at the MP2/W*QZ level.

The spin multiplicities of Ti^+-H_2 , $\text{Ti}^{2+}-\text{H}_2$, and $\text{Ti}^{3+}-\text{H}_2$ are quartet, triplet, and doublet, respectively. The Ti^+-H_2 complex has the $d-\sigma^*$ backdonating bonding orbital (α -HOMO), which does not appear in the occupied regions of the $\text{Ti}^{2+}-\text{H}_2$ and $\text{Ti}^{3+}-\text{H}_2$ complexes as shown in Figure 1. Therefore, the Ti–H distance of the Ti^+-H_2 complex is shorter than those of $\text{Ti}^{2+}-\text{H}_2$ and $\text{Ti}^{3+}-\text{H}_2$ complexes as shown in Table 1. The NBO charges of H atoms (q_{H}) are -0.015 au. In the case of the Ti^+-H_2 complex the α -HOMO is a bonding orbital between a singly occupied d orbital and the unoccupied $\text{H}_2\sigma^*$ orbital. This orbital has the $d-\sigma^*$ backdonation interaction. The second and third α -HOMOs (α -HOMO2 and α -HOMO3) are singly occupied nonbonding d orbitals. The fourth α -HOMO and β -HOMO (α/β -HOMO4) have the weak bonding character between an unoccupied d orbital and the doubly occupied σ orbital of H_2 . This orbital interaction also appears as the third α/β -HOMO (α/β -HOMO3) in $\text{Ti}^{2+}-\text{H}_2$ and as the α/β -HOMO in the $\text{Ti}^{3+}-\text{H}_2$. The α -HOMO and α -HOMO2 of $\text{Ti}^{2+}-\text{H}_2$ are nonbonding orbitals.

The $\text{Ti}-\text{H}_2$ complex has two Ti–H stretching modes (asymmetric and symmetric modes) and one bending mode. As shown in Table 1, the scaled frequency values of asymmetric/symmetric stretching modes at the B3LYP/W*QZ, MP2/W*QZ, and CCSD(T)/W*QZ levels are 1593/1582, 1568/1559, and 1572/1543 cm^{-1} , respectively; those of the bending mode are 573, 458, and 436 cm^{-1} , respectively; the Ti–H distances are 1.759, 1.748, and 1.762 Å, respectively.

The $\text{Ti}^{+2/+3+}-\text{H}_2$ complex has the dihydrogen bond structure by the noncovalent interaction between a Ti ion and an H_2 molecule. In the $\text{Ti}^{4+}-\text{H}_2$ system the electron of H_2 molecule transfers to the Ti^{4+} ion, and the q_{H} is greater than 0.5 au when the H is ~ 2 Å away from the Ti ion; thus the Ti ion and H atoms have all highly positive charges, so that the Ti^{4+} ion does not bind the H_2 molecule or H atoms. A similar situation is found for the $\text{Ti}^{3+}-\text{H}_2$ system at the B3LYP level but not at the MP2 and CCSD(T) levels. At the B3LYP level the ionization energy of H_2 molecule is smaller than the third ionization energy of the titanium atom. Thus, the B3LYP is not reliable for the description of these complexes.

The interaction of Ti^+-H_2 complex was studied experimentally by Bowers' group, who showed that the $4s^1 3d^2$ configuration is more stable than the $3d^3$ configuration.¹⁶ The experimental ΔE_0 of the ground-state Ti^+-H_2 complex ($4s^1 3d^2$) was reported to be 7.5/10.0 kcal/mol more stable than the $3d^2 4s^1$

(ground-state)/ $3d^3$ (excited-state) configuration of Ti^+ . At the B3LYP/W*QZ level, the ground-state configuration of Ti^+ ion is $3d^3$ against the experiment, while at the MP2 and CCSD(T) levels it is $3d^2 4s^1$ in agreement with the experiment. Thus, the B3LYP/W*QZ binding energy ($-\Delta E_0 = 9.90$ kcal/mol) corresponds to the experimental value of 10.0 kcal/mol with respect to the $3d^3$ excited-state configuration instead of the $3d^2 4s^1$ ground-state configuration. The MP2/W*QZ and CCSD(T)/W*QZ binding energies ($-\Delta E_0$: 9.89 and 7.70 kcal/mol, respectively) correspond to the experimental value of 7.5 kcal/mol with respect to the $3d^2 4s^1$ ground-state configuration. Though the MP2/W*QZ value is overestimated in comparison with the experimental value, the CCSD(T)/W*QZ value is in very good agreement with the experiment.

The charge–polarization interaction is a major factor for the binding in these charged complexes. The $\text{Ti}^{3+}-\text{H}_2$ system has the largest polarization interaction among the complexes. The binding energies of the $\text{Ti}^{n+}-\text{H}_2$ complexes ($n = 1-3$) are 9.5, 19.2, and 56.9 kcal/mol, respectively. The main interaction energies arise from the charge(Ti^{n+})–polarization(H_2) interaction. The interaction energies due to H_2 polarization by the positive charge of Ti^{n+} ($n = 1, 2, 3$):

$$\text{polarization energy} = \frac{1}{2}(\text{H}_2\text{polarizability}) \cdot (n \cdot e/r)^2$$

are 8.9, 27.0, and 63.1 kcal/mol, respectively, which are similar to the corresponding total binding energies. In the case of Ti^+-H_2 ($n = 1$), the polarization-driven energy is smaller than the total binding energy, which indicates an additional binding energy for this complexation, i.e., the significant $d-\sigma^*$ backdonation effect. Thus, the Ti–H distance of the Ti^+-H_2 complex is shorter than those of the $\text{Ti}^{2+}-\text{H}_2$ and $\text{Ti}^{3+}-\text{H}_2$ complexes. The ionic radii of Ti^+ , Ti^{2+} , and Ti^{3+} ions are 1.28, 1.00, and 0.81 Å, respectively.²⁹ The ionic radius of Ti^+ is larger than that of Ti^{2+} . However, the Ti^+-H distances are shorter due to the orbital interaction than the $\text{Ti}^{2+}-\text{H}$ distances, as shown in Table 1.

In these charged complexes the H–H stretching frequency (ν_{H_2}) is red-shifted with respect to that of the pure H_2 molecule, as shown in Table 1. The CCSD(T)/W*QZ predicted H–H distances for Ti^+-H_2 , $\text{Ti}^{2+}-\text{H}_2$, and $\text{Ti}^{3+}-\text{H}_2$ are 0.77, 0.77, and 0.84 Å, respectively, with the ν_{H_2} value of 3904, 4037, and 3226 cm^{-1} , respectively. The red-shift is the smallest for the $\text{Ti}^{2+}-\text{H}_2$ complex without $d-\sigma^*$ backdonation, while the red-shift is the largest for the $\text{Ti}^{3+}-\text{H}_2$ complex with strong electrostatic interaction. The asymmetric Ti– H_2 stretching frequency ($\nu_{\text{Ti}-\text{H}_2}^{\text{asym}}$) is the largest in the Ti^+-H_2 complex and the smallest in the $\text{Ti}^{2+}-\text{H}_2$ complex. The CCSD(T)/W*QZ predicted $\nu_{\text{Ti}-\text{H}_2}^{\text{asym}}$ for Ti^+-H_2 , $\text{Ti}^{2+}-\text{H}_2$, and $\text{Ti}^{3+}-\text{H}_2$, are 1057, 783, and 903 cm^{-1} , respectively.

Then, we investigated the structures of dihydrogenated titanium mono- and dications [$\text{Ti}^+(\text{H}_2)_{n=1-7}$ and $\text{Ti}^{2+}(\text{H}_2)_{m=1-9}$]. The geometries were fully optimized at the B3LYP/WTZ and MP2/WTZ levels of theory. An extensive search for the low-lying energy structures including the previously reported ones¹⁶ was made. These structures are shown in Figure 2 for $\text{Ti}^+(\text{H}_2)_n$ and in Figure 3 for $\text{Ti}^{2+}(\text{H}_2)_m$. The dihydrogenated titanium monocations have the spin state of quartet (Q), while the dihydrogenated titanium dications have the triplet state (T). For the notation of each structure, the spin state, the number of H_2 molecules, and the point group of structural symmetry were employed, i.e., Q1-C_{2v} has the spin state of quartet, one H_2 molecule and the point group of C_{2v}. In Figure 3, “T” denotes the triplet state.

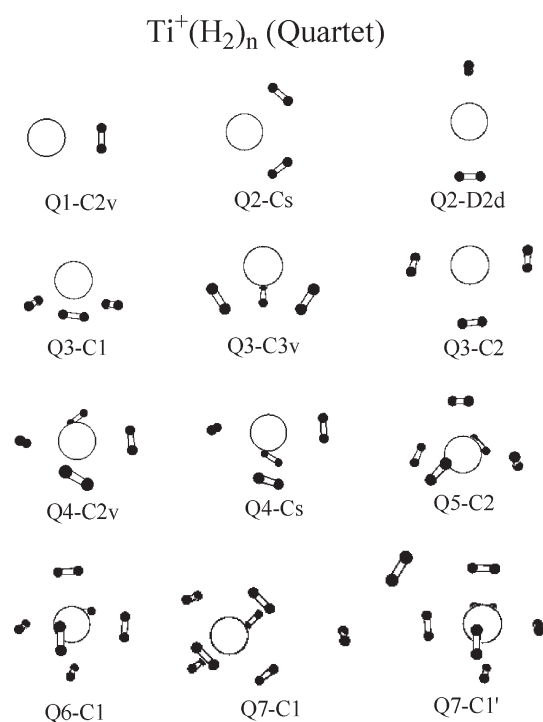


Figure 2. $\text{Ti}^+(\text{H}_2)_{n=1-7}$ structures.

Table 2 lists the binding energies of $\text{Ti}^+(\text{H}_2)_n$ at the B3LYP/WTZ, MP2/WTZ, and CCSD(T)/WTZ levels. In the case of $\text{Ti}^+(\text{H}_2)_2$, the C_s symmetry has the most stable structure (Q2-Cs) at 0 K and room temperature. The D_{2d} structure is a local minimum. For the $\text{Ti}^+(\text{H}_2)_3$ complex, the Q3-C1 conformer has C_{3v} symmetry at the B3LYP/WTZ level as previously reported, but it is transformed into C_1 symmetry at the MP2/WTZ level. At the B3LYP/WTZ level the Q3-C1 is the global minimum, while at the MP2/WTZ and CCSD(T)/WTZ levels the Q3-C3v is the global minimum but almost isoenergetic to the Q3-C1 (within 0.1 kJ/mol at the CCSD(T)/WTZ level). At room temperature the Q3-C1 is the most stable structure at all the levels of calculation. For the $\text{Ti}^+(\text{H}_2)_4$ complex, at the B3LYP/WTZ level the Q4-Cs is the most stable, but at the MP2/WTZ level the Q4-Cs structure transforms into the Q4-C2v structure. In the case of $\text{Ti}^+(\text{H}_2)_5$, the Q5-C2 conformer is the most stable with C_{2v} symmetry.¹² For $\text{Ti}^+(\text{H}_2)_6$, the Q6 has S_4 symmetry at the B3LYP/WTZ level, but C_1 symmetry at the MP2/WTZ level. For $\text{Ti}^+(\text{H}_2)_7$, the Q7-C1 structure which has the coordination 6 + 1 (where 6 and 1 are the numbers of H_2 molecules in the first and second coordination shells, respectively) is the global minimum.

At the CCSD(T)/WTZ level, the $-\Delta E_0$'s of $\text{Ti}^+(\text{H}_2)_{n=1-7}$ are 7.34, 16.16, 24.74, 32.07, 41.99, 48.85, 48.95 kcal/mol, respectively, in good agreement with the experimental values for $n = 1-6$ which are 7.5, 17.2, 26.3, 35.0, 43.2, and 51.9 kcal/mol, respectively. These results indicate that the maximum coordination number of $\text{Ti}^+(\text{H}_2)_n$ is 6 at 0 K. The $-\Delta G^\circ$ (room temperature, 1 atm) for $n = 1-7$ is 3.18, 7.93, 9.42, 11.59, 14.27, 14.15, and 11.09 kcal/mol, respectively, indicating the optimal coordination number of 5–6 at room temperature, as shown in Figure 4. We estimated the approximate complete basis set (aCBS) limit value of the binding energies at the CCSD(T) level, using the extrapolation scheme by utilizing that the electron correlation

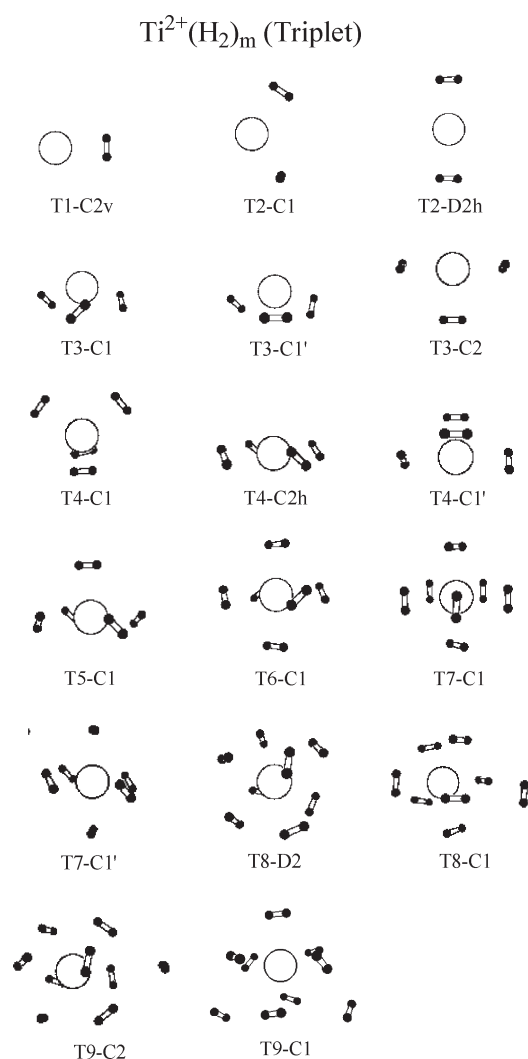


Figure 3. $\text{Ti}^{2+}(\text{H}_2)_{m=1-9}$ structures.

error is proportional to N^{-3} for the (aug)-cc-pVNZ basis set,³⁰ where we used $N = 2, 3$, while N is generally required to use more than 3 and 4.³¹ The estimated CCSD(T)/aCBS $-\Delta E_0$'s of $\text{Ti}^+(\text{H}_2)_1$ and $\text{Ti}^+(\text{H}_2)_6$ are 7.5 and 49.1 kcal/mol. For the Ti^+-H_2 complex the estimated CCSD(T)/aCBS binding energy (ΔE_0) is closer to the experimental value (-7.5 kcal/mol) than the CCSD(T)/WTZ value (-7.3 kcal/mol).

The B3LYP/WTZ, MP2/WTZ, and CCSD(T)/WTZ binding energies of $\text{Ti}^{2+}(\text{H}_2)_{m=1-9}$ are listed in Table 3. The $\text{Ti}^{2+}(\text{H}_2)$ complex has C_{2v} symmetry and the $-\Delta E_0$ is 16.20 kcal/mol at the CCSD(T)/WTZ level, 8.86 kcal/mol larger than that (7.34 kcal/mol) of $\text{Ti}^+(\text{H}_2)$. For the $\text{Ti}^{2+}(\text{H}_2)_2$ complex the T2-C1 structure is the global minimum. The T2-D2h structure has one imaginary frequency at the B3LYP/WTZ level, while T2-D2d has one imaginary frequency at the MP2/WTZ level. In the case of $\text{Ti}^{2+}(\text{H}_2)_3$, the T3-C1 structure is the global minimum, but the T3-C1' structure is nearly iso-energetic within 0.4 kcal/mol at the CCSD(T)/WTZ level. The $\text{Ti}^{2+}(\text{H}_2)_{4-7}$ complexes have C_1 symmetry. The $\text{Ti}^{2+}(\text{H}_2)_8$ complex has the T8-D2 structure (8 + 0). The T8-C1 structure (7 + 1) is slightly less stable. For $\text{Ti}^{2+}(\text{H}_2)_9$, the most stable structure is T9-C2 (8 + 1) at 0 K and T9-C1 (7 + 2) at room temperature, while the (9 + 0) structure is not stable. At the CCSD(T)/WTZ level, the $-\Delta E_0$'s of the

Table 2. Binding Energies (kcal/mol) of $\text{Ti}^+(\text{H}_2)_{n=1-7}$ ^a

$n\text{H}_2$	conformer (sym.) ^b	$(n_1 + n_2)^c$	$-\Delta E_e$	B3LYP/WTZ				MP2/WTZ				CCSD(T)/WTZ ^d			
				$-\Delta E_0$	$-\Delta H_r$	$-\Delta G_r$		$-\Delta E_e$	$-\Delta E_0$	$-\Delta H_r$	$-\Delta G_r$	$-\Delta E_e$	$-\Delta E_0$	$-\Delta H_r$	$-\Delta G_r$
1	Q1-C2v(C_{2v})	(1 + 0)	12.15	10.47	11.57	6.35		12.28	10.39	11.50	6.24	9.20	7.34	8.44	3.18
2	Q2-Cs(C_s)	(2 + 0)	23.81	19.53	21.54	10.75		23.18	18.54	20.51	10.33	20.79	16.16	18.12	7.93
	Q2-D2d(D_{2d})	(2 + 0)	23.16	18.66	20.85	8.23		22.79	17.82	20.06	7.32	19.91	14.94	17.18	4.45
3	Q3-C1(C_{3v} , C_1)	(3 + 0)	35.17	27.88	31.07	12.20		34.76	26.66	30.05	11.77	32.84	24.74	28.13	9.42
	Q3-C3v(C_{3v})	(3 + 0)	35.07	27.77	30.96	12.05		34.89	26.73	30.12	10.80	32.91	24.74	28.13	8.82
	Q3-C2(C_2)	(3 + 0)	34.52	27.26	30.42	11.87		—	—	—	—	—	—	—	—
4	Q4-C2v(C_{2v})	(4 + 0)	44.63	34.37	38.68	12.64		45.03	34.13	38.37	13.67	42.97	32.07	36.30	11.59
	Q4-Cs(C_s)	(4 + 0)	45.42	35.11	39.45	13.73		—	—	—	—	—	—	—	—
5	Q5-C2(C_2)	(5 + 0)	55.20	42.05	47.40	14.16		54.29	39.69	45.36	11.98	56.60	41.99	47.66	14.27
6	Q6-C1(S_6 , C_1)	(6 + 0)	64.46	48.61	54.83	15.50		65.54	46.93	54.17	12.63	67.47	48.85	56.09	14.15
7	Q7-C1(C_1)	(6 + 1)	64.86	48.16	54.21	12.41		66.36	46.95	53.99	9.51	68.36	48.95	56.00	11.09
	Q7-C1'(C_1)	(6 + 1)	64.66	47.89	54.00	11.94		63.91	44.53	51.56	6.65	63.22	43.83	50.86	5.54

^a Binding energy: $E[\text{Ti}^+(\text{H}_2)_n] - E[\text{Ti}^+] - nE[\text{H}_2]$. ^b The conformational symmetries at the B3LYP/WTZ and MP2/WTZ levels are presented in parentheses, respectively; only one group symmetry is given when both symmetries are the same. ^c Both n_1 and n_2 are the numbers of the H_2 molecules in the first and the second solvation shells, respectively. ^d The CCSD(T) data using the WTZ basis set at the MP2/WTZ geometries. The free energy changes of chiral conformers were corrected for chirality by $-RT \ln 2$ (R , gas constant; T , temperature). The experimental $-\Delta E_0$ for $n = 1-6$ is 7.5, 17.2, 26.5, 35.0, 43.2, and 51.9 kcal/mol for the ground-state $4s^1 3d^2$ configuration (ref 16).

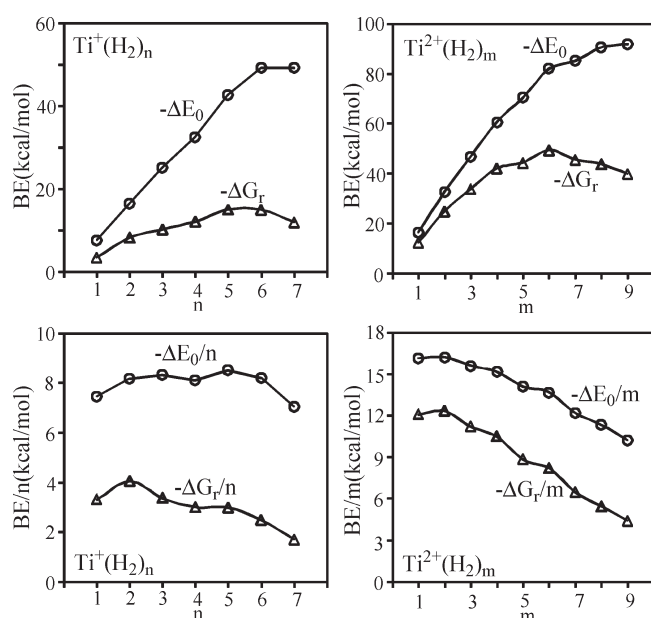


Figure 4. CCSD(T)/WTZ binding energies of the lowest-energy structures of $\text{Ti}^+(\text{H}_2)_n$ and $\text{Ti}^{2+}(\text{H}_2)_m$.

lowest-energy structures of $\text{Ti}^{2+}(\text{H}_2)_{m=1-9}$ are 16.20, 32.53, 46.94, 60.80, 70.70, 82.19, 85.09, 89.60, and 90.73 kcal/mol, respectively. Here, the case for $n = 9$ shows the coordination 8 + 1, while all other lowest-energy structures for $n < 9$ show no secondary coordination. This indicates that the maximum coordination number of $\text{Ti}^{2+}(\text{H}_2)_m$ is 8 at 0 K. The $-\Delta G_r$ for $n = 1-9$ is 12.17, 24.40, (33.80), 41.75, 44.02, 49.00, (45.20), 42.50, and 38.81 kcal/mol, respectively, which indicates the optimal coordination number of 6 at room temperature (Figure 4). Here, the values in parentheses mean that the entropy effect of their two nearly isoenergetic conformers is taken into account.

As shown in Figure 4, for $\text{Ti}^+(\text{H}_2)_{n=1-7}$ and $\text{Ti}^{2+}(\text{H}_2)_{m=1-9}$ at room temperature, the cases of $n = 2$ and $m = 2$ have the largest $-\Delta G_r/n$ and $-\Delta G_r/m$ values (3.97 and 12.20 kcal/mol), respectively. Even though n and m increase, the values of $-\Delta G_r/n$ and $-\Delta G_r/m$ decrease, but the $-\Delta G_r/m$ (4.30 kcal/mol) of $\text{Ti}^{2+}(\text{H}_2)_9$ is larger than $-\Delta G_r/n$ (3.97 kcal/mol) of $\text{Ti}^+(\text{H}_2)_2$. The ionic radius (1.28 Å) of Ti^+ is larger than that (1.00 Å) of Ti^{2+} . However, the Ti^+-H distances are shorter due to the orbital interaction than the $\text{Ti}^{2+}-\text{H}$ distances as shown in Table 1. That is, the solvation sphere of Ti^{2+} is larger than that of Ti^+ ion. The Ti^{2+} ion has more H_2 molecules in the first solvation shell than the Ti^+ ion. Due to the stronger electrostatic interaction by the Ti^{2+} ion, $\text{Ti}^{2+}(\text{H}_2)_m$ have stronger binding energies with a larger coordination number than $\text{Ti}^+(\text{H}_2)_n$.

Table 4 shows the MP2/WTZ NBO charges and selected geometrical parameters of $\text{Ti}^+(\text{H}_2)_{n=1-7}$ and $\text{Ti}^{2+}(\text{H}_2)_{m=1-9}$. For the $\text{Ti}^+(\text{H}_2)_{n=1-7}$ complexes the Q1-C2v and Q2-Cs conformers show electron backdonation from the Ti 3d orbital to H_2 σ^* orbital,¹⁶ and so the NBO charges of Ti ion are larger than +1. For the larger size clusters the electron transfers from the H_2 molecules to the Ti ion. The Ti–H distances for the H_2 molecules in the first coordination shell are around 2.0 Å, while those for the H_2 molecules in the second coordination shell are over 4.0 Å. The H–H distances of H_2 molecules in the complexes are elongated in comparison with that of the pure H_2 molecule. For the $\text{Ti}^{2+}(\text{H}_2)_m$ complexes, the electron transfers from the H_2 molecules to the Ti ion, without the d– σ^* backdonation. The Ti–H distances of $\text{Ti}^{2+}(\text{H}_2)_m$ are longer than those of $\text{Ti}^+(\text{H}_2)_n$ involved in the d– σ^* backdonation, while the H–H distances of H_2 molecules in $\text{Ti}^{2+}(\text{H}_2)_m$ are shorter than those in $\text{Ti}^+(\text{H}_2)_n$. Figure 5 shows the MP2/WTZ NBO charges of titanium ions in the ΔE_0 -based lowest-energy structures of $\text{Ti}^+(\text{H}_2)_n$ and $\text{Ti}^{2+}(\text{H}_2)_m$. The charge transfer from hydrogen molecules to the titanium ion increases up to $n = 6$ and $m = 7$ where the charge transfers are almost saturated. The Ti^+ ion accepts charge by -0.58 au in Q6-C1, while the Ti^{2+} ion accepts charge by -0.63 au in T6-C1. In $\text{Ti}^+(\text{H}_2)_n$ the charge ($q_{\text{NBO}}^{\text{Ti}}$)

Table 3. Binding Energies (kcal/mol) of $\text{Ti}^{2+}(\text{H}_2)_{m=1-9}^a$

$m\text{H}_2$	conformer (sym.)	$(n_1 + n_2)$	B3LYP/WTZ				MP2/WTZ				CCSD(T)/WTZ			
			$-\Delta E_e$	$-\Delta E_0$	$-\Delta H_r$	$-\Delta G_r$	$-\Delta E_e$	$-\Delta E_0$	$-\Delta H_r$	$-\Delta G_r$	$-\Delta E_e$	$-\Delta E_0$	$-\Delta H_r$	$-\Delta G_r$
1	T1-C2v(C_{2v})	(1 + 0)	20.37	18.92	19.98	14.89	17.49	15.85	16.92	11.81	17.83	16.20	17.28	12.17
2	T2-C1(C_1)	(2 + 0)	40.99	37.49	39.13	30.22	35.84	31.83	33.60	24.10	36.54	32.53	34.32	24.40
	T2-D2h(D_{2h}) ^b	(2 + 0)	39.12	35.38	37.79	24.84	35.70	31.74	33.49	22.87	36.35	32.41	34.15	23.54
3	T3-C1(C_1)	(3 + 0)	59.05	53.19	55.65	40.05	52.32	45.84	48.39	32.70	53.42	46.94	49.47	33.39
	T3-C1'(C_1)	(3 + 0)	57.96	51.47	54.39	37.17	52.31	45.81	48.39	32.65	53.37	46.87	49.45	33.32
	T3-C2(C_{2v})	(3 + 0)	53.68	47.10	49.98	32.49	—	—	—	—	—	—	—	—
4	T4-C1(C_1)	(4 + 0)	75.67	67.58	70.71	49.39	68.22	59.29	62.63	40.67	69.72	60.80	64.13	41.75
	T4-C2h(C_{2h})	(4 + 0)	73.67	65.03	68.59	44.46	66.40	56.70	60.65	35.53	67.97	58.27	62.21	37.09
	T4-C1b(C_1)	(4 + 0)	70.93	61.55	65.44	42.31	63.92	53.45	57.69	32.98	66.40	55.93	60.16	35.04
5	T5-C1(C_{3v})	(5 + 0)	88.81	77.11	81.95	50.13	81.32	68.94	73.81	42.68	83.08	70.70	75.57	44.02
6	T6-C1(C_1)	(6 + 0)	102.53	87.86	93.87	54.65	94.90	79.64	85.63	46.86	97.44	82.19	88.17	49.00
7	T7-C1(C_{2v})	(7 + 0)	110.10	92.41	99.57	52.69	103.34	81.83	90.35	41.99	106.60	85.09	93.59	44.81
	T7-C1'(C_1)	(6 + 1)	104.95	88.68	95.04	50.62	97.85	80.86	87.31	42.66	100.50	83.53	89.96	44.91
8	T8-D2(D_2)	(8 + 0)	113.36	93.77	101.63	47.44	107.86	86.39	95.04	39.28	111.07	89.60	98.23	42.50
	T8-C1(C_1)	(7 + 1)	112.39	93.25	100.68	50.30	105.75	84.38	92.74	39.11	109.37	88.00	96.37	42.33
9	T9-C2(C_2)	(8 + 1)	115.21	94.09	102.25	43.19	110.53	87.41	96.48	34.82	113.86	90.73	99.81	38.15
	T9-C1(C_1)	(7 + 2)	114.66	93.91	101.73	44.60	108.78	86.33	94.84	35.69	112.33	89.87	98.37	38.81

^a See the footnote of Table 2. ^b Though this structure is a transition state at B3LYP/WTZ, it is a minimum at MP2/WTZ.

Table 4. MP2/WTZ NBO Charges (q_{NBO}) and Geometrical Parameters (Å) of $\text{Ti}^+(\text{H}_2)_n$ and $\text{Ti}^{2+}(\text{H}_2)_m$ ^a

$\text{Ti}^+(\text{H}_2)_n$				$\text{Ti}^{2+}(\text{H}_2)_m$			
conf.	$q_{\text{NBO}}^{\text{Ti}}$	$r_{\text{Ti-H}}^{\text{av}}$	$r_{\text{HH}}^{\text{av}}$	conf.	$q_{\text{NBO}}^{\text{Ti}}$	$r_{\text{Ti-H}}^{\text{av}}$	$r_{\text{HH}}^{\text{av}}$
Q1-C2v	1.03	1.983	0.765	T1-C2v	1.98	2.151	0.765
Q2-Cs	1.02	1.983	0.767	T2-C1	1.91	2.135	0.763
Q3-C1	0.95	1.976	0.769	T2-D2h	1.92	2.148	0.762
Q3-C3v	0.95	1.976	0.769	T3-C1	1.82	2.139	0.761
Q4-C2v	0.83	2.013	0.765	T3-C1'	1.82	2.139	0.761
Q5-C2	0.66	2.001	0.767	T4-C1	1.70	2.141	0.760
Q6-C1	0.42	2.002	0.766	T5-C1	1.56	2.137	0.760
Q7-C1	0.42	2.002	0.766	T6-C1	1.37	2.134	0.759
	(4.087)	(0.739)		T7-C1	1.14	2.129	0.759
				T8-D2	1.10	2.224	0.753
				T9-C2	1.08	2.223	0.753
						(3.600)	(0.742)
				T9-C1	1.26	2.150	0.757
						(3.481)	(0.743)

^a $q_{\text{NBO}}^{\text{Ti}}$ is the NBO charge of the Ti ion; $r_{\text{Ti-H}}^{\text{av}}$ is the average Ti–H distance; and $r_{\text{HH}}^{\text{av}}$ is the average H–H distance of the first-shell H_2 molecules. The data in parentheses are of the secondary shell H_2 molecules. The H–H distance of the pure H_2 is 0.738 Å at the MP2/WTZ level.

converges to +0.42 au as the number of H_2 molecules increases up to $n = 6$. In $\text{Ti}^{2+}(\text{H}_2)_m$ the charge converges to +1.14 au as the number of H_2 molecules increases up to $m = 7$, as shown in Figure 5. At the MP2/WTZ level the average $\text{Ti}^+ \text{--} \text{H}$ distances in Q6-C1 and Q7-C1 are 2.002 Å, while the average $\text{Ti}^{2+} \text{--} \text{H}$ distances in T6-C1 is 2.134 Å. The shortest intermolecular distances between the nearest-neighboring H_2 centers in the first solvation shells of Q6-C1 and Q7-C1 are 2.65 Å. The

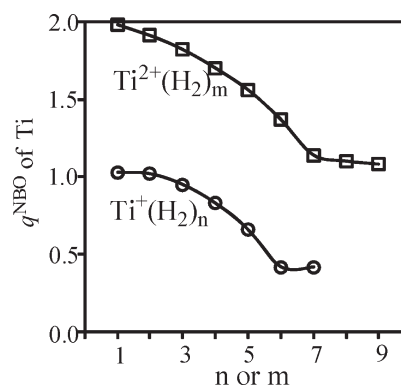


Figure 5. MP2/WTZ NBO charge (q_{NBO}) of the titanium ion in the ΔE_0 -based lowest-energy structures of $\text{Ti}^+(\text{H}_2)_n$ and $\text{Ti}^{2+}(\text{H}_2)_m$.

shortest distances between the nearest-neighboring H_2 centers in the first solvation shells of T6-C1, T7-C1, T8-D2, and T9-C2 are 2.86, 2.48, 2.53, and 2.53 Å, respectively. The shortest $\text{H}_2 \text{--} \text{H}_2$ distances for hepta-, octa-, and nonacoordinated systems are already small enough to accommodate an extra H_2 .

The vibrational frequencies of $\text{Ti}^+(\text{H}_2)_n$ were calculated at the B3LYP/WTZ and MP2/WTZ levels. Table 5 lists the MP2 (B3LYP) frequencies scaled by 0.975 (0.966) to match the frequency of pure H_2 with respect to the experimental value (4401 cm^{-1})²⁸ and their IR intensities. The frequencies and their intensities of $\text{Ti}^{2+}(\text{H}_2)_m$ are listed in Table 6. Generally, in the case of electrostatic energy driven interaction systems the H–H stretching frequencies increase and the asymmetric Ti ion– H_2 stretching frequencies decrease with the increasing number of H_2 molecules. However, this trend does not appear due to the complex orbital interactions, especially in the $\text{Ti}^+(\text{H}_2)_n$ cases. The $\text{Ti}^+(\text{H}_2)_n$ complexes have orbital interactions due to the $d \text{--} \sigma^*$ backdonation in addition to weak electrostatic interactions,

Table 5. Selected Frequencies and IR Intensities in Subscripts (10 km/mol) of $\text{Ti}^+(\text{H}_2)_n$ at the MP2/WTZ (B3LYP/WTZ) level^a

<i>n</i>	conformer	H–H stretch	asym. $\text{Ti}^+ - \text{H}_2$ stretch in the first shell
1	Q1-C2v	3910 ₁₃ (3841 ₁₃)	1051 (1027)
2	Q2-Cs	3884 ₆ 3900 ₁₈ (3859 ₁₈ 3863 ₅)	1070 1083 (1033 1037)
3	Q3-C1	3855 ₃ 3869 ₁₆ 3870 ₁₆ (3875 ₁₃ 3875 ₁₃ 3881 ₂)	1078 1102 1102 (1031 1043 1043)
	Q3-C3v	3860 ₁ 3866 ₂₀ 3866 ₂₀ (3878 ₁₅ 3878 ₁₅ 3886 ₁)	1100 1100 1115 (1037 1037 1045)
4	Q4-C2v	3930 ₀ 3935 ₁₈ 3935 ₁₈ 3948 ₀ (3937 ₂₈ 3938 ₂₃ 3938 ₀ 3941 ₀)	1033 1057 1057 1059 (1001 1003 1007 1007)
5	Q5-C2	3864 ₅ 3915 ₂ 3920 ₁₅ 3926 ₁₅ 3932 ₀ (3920 ₅ 3951 ₀ 3952 ₁₃ 3954 ₁₁ 3956 ₁)	1058 1068 1071 1073 1123 (999 1003 1004 1006 1035)
6	Q6-C1	3910 ₀ 3915 ₅ 3916 ₅ 3924 ₇ 3928 ₅ 3929 ₅ (3968 ₀ 3968 ₁ 3973 ₈ 3973 ₈ 3973 ₈ 3980 ₀)	1089 1089 1090 1090 1092 1093 (994 996 996 999 1000 1000)
7	Q7-C1	3910 ₁ 3915 ₆ 3919 ₂ 3923 ₇ 3929 ₆ 3934 ₄ 4380 ₁ (3966 ₂ 3968 ₁ 3972 ₇ 3973 ₈ 3976 ₆ 3980 ₁ 4384 ₁)	1088 1089 1091 1092 1092 1094 (996 997 998 1001 1001 1002)

^a MP2 (B3LYP) frequencies are scaled by 0.975 (0.966) to match the frequency of pure H_2 with respect to the experimental value (4401 cm^{-1}) from ref 28. The intensities of $\text{Ti}^+ - \text{H}_2$ stretches are omitted due to their small values.

Table 6. Selected Frequencies and IR Intensities in Subscripts (10 km/mol) of $\text{Ti}^{2+}(\text{H}_2)_m$ at the MP2/WTZ (B3LYP/WTZ) Level^a

<i>m</i>	conformer	H–H stretch	asym. $\text{Ti}^{2+} - \text{H}_2$ stretch
1	T1-C2v	4033 ₁₅ (3965 ₁₉)	784 (760)
2	T2-C1	4058 ₂₁ 4065 ₉ (4003 ₂₆ 4014 ₉)	794 797 (765 771)
3	T3-C1	4079 ₁₈ 4079 ₁₈ 4087 ₃ (4028 ₂₃ 4028 ₂₃ 4042 ₃)	799 802 804 (775 776 778)
	T3-C1'	4078 ₁₈ 4078 ₁₈ 4086 ₃ (4023 ₁₃ 4023 ₂₀ 4033 ₇)	796 797 804 (791 795 797)
4	T4-C1	4090 ₁₇ 4091 ₁₅ 4091 ₁₅ 4100 ₀ (4055 ₁₉ 4055 ₁₇ 4056 ₁₇ 4070 ₀)	797 803 807 809 (776 778 782 786)
5	T5-C1	4086 ₉ 4095 ₁₈ 4097 ₁₁ 4098 ₂ 4100 ₅ (4055 ₁₀ 4068 ₂₁ 4071 ₁₈ 4073 ₁ 4079 ₁)	792 812 814 826 833 (787 793 797 799 821)
6	T6-C1	4096 ₁₃ 4096 ₅ 4096 ₁₈ 4098 ₀ 4098 ₀ 4101 ₁₄ (4078 ₁₉ 4078 ₁₉ 4082 ₀ 4082 ₁ 4082 ₁₄ 4086 ₀)	786 813 818 818 827 827 (796 806 806 807 811 812)
7	T7-C1	4074 ₀ 4077 ₁₂ 4110 ₀ 4110 ₀ 4114 ₁₉ 4115 ₁₉ 4120 ₀ (4082 ₁₅ 4083 ₀ 4109 ₂ 4111 ₉ 4114 ₁₇ 4115 ₁₃ 4123 ₂)	821 822 846 859 860 861 862 (774 775 778 781 792 810 811)
8	T8-D2	4189 ₀ 4191 ₂₁ 4192 ₁₇ 4192 ₂₀ 4193 ₂ 4193 ₁ 4193 ₄ 4195 ₀ (4179 ₂₄ 4179 ₂₄ 4179 ₂₃ 4179 ₀ 4181 ₁ 4182 ₀ 4182 ₁ 4190 ₀)	687 691 691 696 701 704 704 707 (695 695 697 698 702 704 705 706)
9	T9-C2	4181 ₉ 4183 ₉ 4193 ₈ 4194 ₁₂ 4196 ₃ 4197 ₉ 4197 ₉ 4199 ₄ 4336 ₄ (4169 ₁₃ 4172 ₁₃ 4179 ₈ 4181 ₂ 4185 ₁₈ 4185 ₁₂ 4189 ₅ 4194 ₀ 4314 ₅)	684 690 695 699 704 707 729 739 (694 696 702 703 708 709 734 736)
	T9-C1	4100 ₀ 4100 ₁₅ 4133 ₀ 4134 ₁₁ 4138 ₉ 4140 ₇ 4143 ₁₀ 4323 ₇ 4323 ₄ (4070 ₁₆ 4072 ₀ 4100 ₆ 4106 ₁₅ 4116 ₄ 4119 ₁₅ 4124 ₃ 4328 ₉ 4328 ₅)	774 793 800 808 819 836 838 (772 782 790 825 830 839 840)

^a See the footnote of Table 5.

whereas the $\text{Ti}^{2+}(\text{H}_2)_m$ complexes have relatively strong electrostatic interactions. Owing to the d- σ^* backdonation, the Ti ion–H distances of $\text{Ti}^+(\text{H}_2)_n$ are shorter than those of $\text{Ti}^{2+}(\text{H}_2)_m$. Since the H–H distances of H_2 molecules in $\text{Ti}^+(\text{H}_2)_n$ complexes are longer than those in $\text{Ti}^{2+}(\text{H}_2)_m$ due to the d- σ^* backdonation, the H–H stretching frequencies of $\text{Ti}^+(\text{H}_2)_n$ are smaller (more shifted in comparison with the frequency of pure H_2 molecule) than those of $\text{Ti}^{2+}(\text{H}_2)_m$. On the other hand, the asymmetric $\text{Ti}^{2+} - \text{H}_2$ stretching frequencies of $\text{Ti}^{2+}(\text{H}_2)_m$ are smaller than the asymmetric $\text{Ti}^+ - \text{H}_2$ stretching frequencies of $\text{Ti}^+(\text{H}_2)_n$. The B3LYP/WTZ IR spectra for the H–H stretching frequencies of the ΔE_0 -based lowest-energy structures of $\text{Ti}^+(\text{H}_2)_n$ and $\text{Ti}^{2+}(\text{H}_2)_m$ are shown in Figure 6. The red shifts of H–H stretching frequencies decrease with increasing number of hydrogen molecules in both $\text{Ti}^+(\text{H}_2)_n$ and $\text{Ti}^{2+}(\text{H}_2)_m$. The red shift becomes minimal at $n = 6$ in the $\text{Ti}^+(\text{H}_2)_n$ complexes and at $m = 8$ in the $\text{Ti}^{2+}(\text{H}_2)_m$ complexes.

At 373 K, ΔG_{373} 's of Q6-C1, T6-C1, T7-C1, T7-C1', and T8-D2 were calculated to be –20.82, –39.67, –33.03, –34.11, and –28.49 kcal/mol, based on the CCSD(T) energies with the MP2 thermal energy corrections. These binding free energies are most suitable to store and release hydrogen molecules. As Ti^{n+} cations should be neutralized with anions in real hydrogen storage materials, researchers have been trying to design optimal systems. Transition metals have the tendency to aggregate among themselves, resulting in the reduction of the hydrogen storage capacity. Thus, to stabilize the dispersed transition metals, they can be embedded in frameworks or decorated on the substrate. To bind hydrogen directly, the Ti cations should be in the (I–III) oxidation states, not in the (IV) oxidation state. Hypothetical studies of Ti-decorated bulkyballs ($\text{Ti(I)}_{12}\text{B}_{24}\text{C}_{36}$, 8.6 wt % H_2),³² Ti(I–III) –graphene oxide (4.9 wt % H_2),³³ Ti(I) –nanotubes (5–8 wt % H_2),³⁴ Ti(I) –ethane-diol (13 wt % H_2),³⁵ and Ti-substituted boranes ($\text{Ti(II)}_n\text{–B}_m\text{H}_m$, maximum 10.0 wt % H_2)³⁶ have been carried out. The

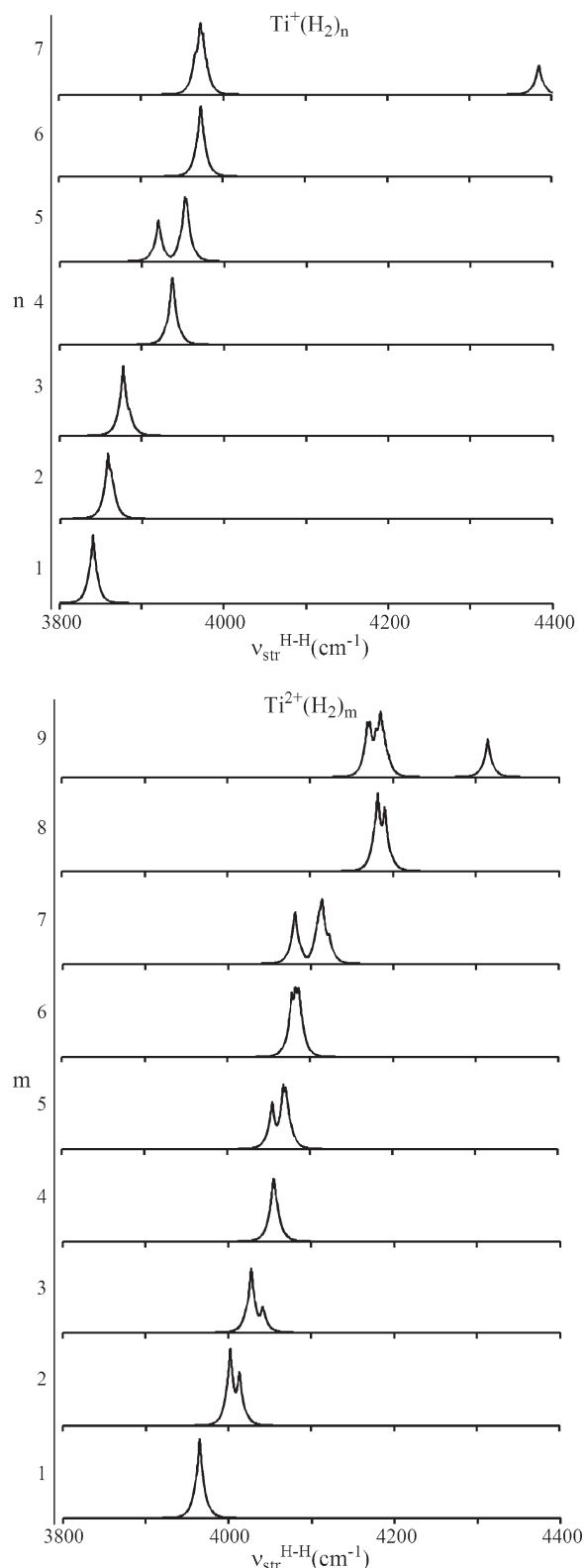


Figure 6. B3LYP/WTZ vibrational frequencies for the H–H stretching modes of the ΔE_0 -based lowest-energy structures of $\text{Ti}^+(\text{H}_2)_n$ and $\text{Ti}^{2+}(\text{H}_2)_m$.

$\text{Ti}^{2+}(\text{H}_2)_8$ complexation (25.2 wt %) would help design effective hydrogen storage materials by Ti-decoration on or Ti-dispersion in graphene derivatives, organic π systems with

strongly electronegative substituents, or polymer–graphene hybrid materials.

IV. CONCLUDING REMARKS

The neutral and multiply charged titanium– H_2 systems ($\text{Ti}-\text{H}_2$, Ti^+-H_2 , $\text{Ti}^{2+}-\text{H}_2$, $\text{Ti}^{3+}-\text{H}_2$ and $\text{Ti}^{4+}-\text{H}_2$) were calculated using the B3LYP, MP2 and CCSD(T) methods with the W*QZ basis set. The neutral $\text{Ti}-\text{H}_2$ system has the covalent-bonded dihydride configuration with strong $d-\sigma^*$ backdonation. The Ti^+-H_2 , $\text{Ti}^{2+}-\text{H}_2$ and $\text{Ti}^{3+}-\text{H}_2$ complexes have the non-covalent-bonded dihydrogen configurations with the electrostatic interaction, resulting in electron donation from the H_2 σ orbital to the metal which stabilizes the ion charge. Especially for the Ti^+-H_2 complex the empty 4s orbital plays a crucial role in the stability. The B3LYP calculation fails to describe the binding between a titanium trication (Ti^{3+}) and a hydrogen molecule. The Ti^{4+} ion does not bind a H_2 molecule. The predicted binding energy of the Ti^+-H_2 complex is in good agreement with the experimental value. Among the Ti^+-H_2 , $\text{Ti}^{2+}-\text{H}_2$, and $\text{Ti}^{3+}-\text{H}_2$ complexes, the Ti^+-H_2 system has a characteristic bonding orbital with the $d-\sigma^*$ backdonation which leads to the shortest Ti–H distance and the highest Ti– H_2 asymmetric stretching frequency; the $\text{Ti}^{3+}-\text{H}_2$ system has the strong electrostatic interaction; the $\text{Ti}^{2+}-\text{H}_2$ system has the longest Ti–H distance, resulting in the smallest red shift in the H–H stretching frequency and the smallest Ti– H_2 asymmetric stretching frequency.

Then the coordination structures of $\text{Ti}^+(\text{H}_2)_{n=1-7}$ and $\text{Ti}^{2+}(\text{H}_2)_{m=1-9}$ were studied at the B3LYP/WTZ, MP2/WTZ, and CCSD(T)/WTZ levels of theory. At low temperatures the most stable structures of $\text{Ti}^+(\text{H}_2)_{n=1-7}$ are Q1-C2v (1 + 0), Q2-Cs (2 + 0), Q3-C3v (3 + 0), Q4-C2v (4 + 0), Q5-C2 (5 + 0), Q6-C1 (6 + 0), and Q7-C1 (6 + 1), while at room temperature the most stable structures are Q1-C2v (1 + 0), Q2-Cs (2 + 0), Q3-C1 (3 + 0), Q4-C2v (4 + 0), Q5-C2 (5 + 0), Q6-C1 (6 + 0), and Q7-C1b (6 + 1). For the $\text{Ti}^{2+}(\text{H}_2)_{m=1-9}$ complexes, T1-C2v (1 + 0), T2-C1 (2 + 0), T3-C1 (3 + 0), T4-C1 (4 + 0), T5-C1 (5 + 0), T6-C1 (6 + 0), T7-C1 (7 + 0), T8-D2 (8 + 0), and T9-C2 (8 + 1) are the most stable structures at low temperatures, while T1-C2v (1 + 0), T2-C1 (2 + 0), T3-C1/T3-C1 (3 + 0), T4-C1 (4 + 0), T5-C1 (5 + 0), T6-C1 (6 + 0), T7-C1/T7-C1' (7 + 0), T8-D2 (8 + 0) and T9-C2 (7 + 2) are the most stable structures at room temperature. The $\text{Ti}^+(\text{H}_2)_n$ complexes have orbital interactions due to the $d-\sigma^*$ electron backdonation in addition to weak electrostatic interactions, while the $\text{Ti}^{2+}(\text{H}_2)_m$ complexes have relatively strong electrostatic interactions. Thus, the binding energies of $\text{Ti}^{2+}(\text{H}_2)_m$ complexes are larger than those of $\text{Ti}^+(\text{H}_2)_n$. However, the Ti–H distances of $\text{Ti}^+(\text{H}_2)_n$ are shorter than those of $\text{Ti}^{2+}(\text{H}_2)_m$, and the H–H distances of H_2 molecules in $\text{Ti}^+(\text{H}_2)_n$ complexes are longer than those in $\text{Ti}^{2+}(\text{H}_2)_m$. Thus, the H–H stretching frequencies of $\text{Ti}^+(\text{H}_2)_n$ are smaller than those of $\text{Ti}^{2+}(\text{H}_2)_m$, whereas the asymmetric $\text{Ti}^{2+}-\text{H}_2$ stretching frequencies of $\text{Ti}^{2+}(\text{H}_2)_m$ are smaller than the asymmetric Ti^+-H_2 stretching frequencies of $\text{Ti}^+(\text{H}_2)_n$. For $\text{Ti}^+(\text{H}_2)_n$ and $\text{Ti}^{2+}(\text{H}_2)_m$ it is possible to have up to the hexacoordination and octacoordination at very low temperatures, respectively, while they favor penta- to hexacoordination and hexacoordination, respectively, at room temperature and 1 atm. This coordination structure would be important information for the design of hydrogen storage material of Ti complexes. Indeed, many Ti-decorated systems have been studied for their H_2 storage properties.^{10,32–36} From this study, we find that the titanium atoms

need to have positive charges (preferentially doubly charged state which allows the primary coordination number of 6 at ambient conditions and up to 8 at very low temperatures near 0 K) for better H₂ storage.

AUTHOR INFORMATION

Corresponding Author

*E-mail: kim@postech.ac.kr.

ACKNOWLEDGMENT

This work is affectionately dedicated to Professor Bernd Brutschy, an outstanding scientist, on the occasion of his 65th birthday. This work was supported by NRF (WCU: R32-2008-000-10180-0, BK21, National honor scientist program) and KISTI (KSC-2008-K08-0002).

REFERENCES

- Coontz, R.; Hanson, B. *Science* **2004**, *305*, 957.
- Orimo, S.-I.; Nakamori, Y.; Eliseo, J. R.; Züttel, A.; Jensen, C. M. *Chem. Rev.* **2007**, *107*, 4111–4132.
- Marder, C. T. B. *Angew. Chem., Int. Ed.* **2007**, *46*, 8116–8118.
- (a) Xiong, Z.; Yong, C. K.; Wu, G.; Chen, P.; Shaw, W.; Karkamkar, A.; Autrey, T.; Jones, M. O.; Johnson, S. R.; Edwards, P. P.; David, W. I. F. *Nat. Mater.* **2008**, *7*, 138–141. (b) Kim, D. Y.; Singh, N. J.; Lee, H. M.; Kim, K. S. *Chem.—Eur. J.* **2009**, *15*, 5598. (c) Kim, D. Y.; Lee, H. M.; Seo, J.; Shin, S. K.; Kim, K. S. *Phys. Chem. Chem. Phys.* **2010**, *12*, 5446.
- U. S. Department of Energy Hydrogen Program Annual Merit Review Proceedings, Arlington, VA, May 18–22, 2009; http://www.hydrogen.energy.gov/annual_review09_proceedings.html.
- (a) Rowsell, J. L. C.; Yaghi, O. M. *Angew. Chem.* **2005**, *117*, 4748–4758. (b) Rowsell, J. L. C.; Yaghi, O. M. *Angew. Chem., Int. Ed.* **2005**, *44*, 4670–4679. (c) Han, S. S.; Furukawa, H.; Yaghi, O. M.; Goddard, W. A., III *J. Am. Chem. Soc.* **2008**, *130*, 11580–11581.
- Kubas, G. J. *Chem. Rev.* **2007**, *107*, 4152.
- (a) Kim, Y. H.; Zhao, Y. F.; Williamson, A.; Heben, M. J.; Zhang, S. B. *Phys. Rev. Lett.* **2006**, *96*, 016102. (b) Zhao, Y.; Kim, Y.-H.; Dillan, A. C.; Heben, M. J.; Zhang, S. B. *Phys. Rev. Lett.* **2005**, *94*, 155504.
- (a) Sun, Q.; Wang, Q.; Jena, P.; Kawazoe, Y. *J. Am. Chem. Soc.* **2005**, *127*, 14582. (b) Kiran, B.; Kandalam, A. K.; Jena, P. *J. Chem. Phys.* **2006**, *124*, 224703. (c) Zhou, W.; Yildirim, T.; Durgun, E.; Ciraci, S. *Phys. Rev. B* **2007**, *76*, 085434. (d) Weck, P. F.; Kumar, T. J. D.; Kim, E.; Balakrishnan, N. *J. Chem. Phys.* **2007**, *126*, 094703. (e) Kim, T. S.; Kim, K. J.; Jo, S. K.; Lee, J. *J. Phys. Chem. B* **2008**, *112*, 16431. (f) Bhattacharya, S.; Majumder, C.; Das, G. P. *J. Phys. Chem. C* **2008**, *112*, 17487. (g) Okamoto, Y. *J. Phys. Chem. C* **2008**, *112*, 17721. (h) Barman, S.; Sen, P.; Das, G. P. *J. Phys. Chem. C* **2008**, *112*, 19963. (i) Bhattacharya, S.; Majumder, C.; Das, G. P. *J. Phys. Chem. C* **2009**, *113*, 15783.
- Hamaed, A.; Trudeau, M.; Antonelli, D. M. *J. Am. Chem. Soc.* **2008**, *130*, 6992.
- Kim, Y.-H.; Sun, Y. Y.; Choi, W. I.; Kang, J.; Zhang, S. B. *Phys. Chem. Chem. Phys.* **2009**, *11*, 11400.
- Park, M. H.; Lee, Y. S. *Chem. Phys. Lett.* **2010**, *488*, 7.
- (a) Tarakeswar, P.; Kumar, T. J. D.; Balakrishnan, N. *J. Phys. Chem.* **2008**, *112*, 2846. (b) Kumar, T. J. D.; Tarakeswar, P.; Balakrishnan, N. *J. Chem. Phys.* **2008**, *128*, 194714. (c) Tarakeswar, P.; Kumar, T. J. D.; Balakrishnan, N. *J. Chem. Phys.* **2009**, *130*, 114301.
- (a) Kim, K. S.; Suh, S. B.; Kim, J. C.; Hong, B. H.; Lee, E. C.; Yun, S.; Tarakeswar, P.; Lee, J. Y.; Kim, Y.; Ihm, H.; Kim, H. G.; Lee, J. W.; Kim, J. K.; Lee, H. M.; Kim, D.; Cui, C.; Youn, S. J.; Chung, H. Y.; Choi, H. S.; Lee, C.-W.; Cho, S. J.; Jeong, S.; Cho, J.-H. *J. Am. Chem. Soc.* **2002**, *124*, 14268. (b) Singh, N. J.; Lee, H. M.; Hwang, I.-C.; Kim, K. S. *Supramol. Chem.* **2007**, *19*, 321. (c) Singh, N. J.; Lee, E. C.; Choi, Y. C.; Lee, H. M.; Kim, K. S. *Bull. Chem. Soc. Jpn.* **2007**, *80*, 1437. (d) Lee, J. Y.; Hong, B. H.; Kim, W. Y.; Min, S. K.; Kim, Y.; Jouravlev, M. V.; Bose, R.; Kim, K. S.; Hwang, I.-C.; Kaufman, L. J.; Wong, C. W.; Kim, P.; Kim, K. S. *Nature* **2009**, *460*, 498. (e) Chellappan, K.; Singh, N. J.; Hwang, I.-C.; Lee, J. W.; Kim, K. S. *Angew. Chem., Int. Ed.* **2005**, *44*, 2899.
- Bushnell, J. E.; Kemper, P. R.; Maitre, P.; Bowers, M. T. *J. Am. Chem. Soc.* **1994**, *116*, 9710.
- Bushnell, J. E.; Maitre, P.; Kemper, P. R.; Bowers, M. T. *J. Chem. Phys.* **1997**, *106*, 10153.
- Bushnell, J. E.; Kemper, P. R.; Bowers, M. T. *J. Phys. Chem.* **1993**, *97*, 11628. (b) Maitre, P.; Bauschlicher, C. W., Jr. *J. Phys. Chem.* **1995**, *99*, 6836.
- Bauschlicher, C. W., Jr.; Partridge, H.; Langhoff, S. R. *J. Phys. Chem.* **1992**, *96*, 2475.
- Weis, P.; Kemper, P. R.; Bowers, M. T. *J. Phys. Chem.* **1997**, *101*, 2809.
- Bushnell, J. E.; Kemper, P. R.; Bowers, M. T. *J. Phys. Chem.* **1995**, *99*, 15602.
- (a) Kemper, P. R.; Bushnell, J.; von Helden, G.; Bowers, M. T. *J. Phys. Chem.* **1993**, *97*, 52. (b) Bauschlicher, C. W., Jr.; Maitre, P. *J. Phys. Chem.* **1995**, *99*, 3444.
- (a) Kemper, P. R.; Weis, P.; Bowers, M. T.; Maitre, P. *J. Am. Chem. Soc.* **1998**, *120*, 13494. (b) Manard, M. J.; Bushnell, J. E.; Bernstein, S. L.; Bowers, M. T. *J. Phys. Chem. A* **2002**, *106*, 10027.
- Liu, C. S.; Zeng, Z. *Phys. Rev. B* **2009**, *79*, 245419.
- Frisch, M. J.; Trucks, G. W.; Schlegel, H. B.; Scuseria, G. E.; Robb, M. A.; Cheeseman, J. R.; Zakrzewski, V. G.; Montgomery, J. A., Jr.; Stratmann, R. E.; Burant, J. C.; Dapprich, S.; Millam, J. M.; Daniels, A. D.; Kudin, K. N.; Strain, M. C.; Farkas, O.; Tomasi, J.; Barone, V.; Cossi, M.; Cammi, R.; Mennucci, B.; Pomelli, C.; Adamo, C.; Clifford, S.; Ochterski, J.; Petersson, G. A.; Ayala, P. Y.; Cui, Q.; Morokuma, K.; Salvador, P.; Dannenberg, J. J.; Malick, D. K.; Rabuck, A. D.; Raghavachari, K.; Foresman, J. B.; Cioslowski, J.; Ortiz, J. V.; Baboul, A. G.; Stefanov, B. B.; Liu, G.; Liashenko, A.; Piskorz, P.; Komaromi, I.; Gomperts, R.; Martin, R. L.; Fox, D. J.; Keith, T.; Al-Laham, M. A.; Peng, C. Y.; Nanayakkara, A.; Challacombe, M.; Gill, P. M. W.; Johnson, B.; Chen, W.; Wong, M. W.; Andres, J. L.; Gonzalez, C.; Head-Gordon, M.; Replogle, E. S.; Pople, J. A. *Gaussian 03*, revision A.1; Gaussian, Inc.: Pittsburgh, PA, 2003.
- Lee, S. J.; Chung, H. Y.; Kim, K. S. *Bull. Korean Chem. Soc.* **2004**, *25*, 1061.
- (a) Wachters, A. J. H. *J. Chem. Phys.* **1970**, *52*, 1033. (b) Bauschlicher, C. W., Jr.; Langhoff, S. R.; Barnes, L. A. *J. Chem. Phys.* **1989**, *91*, 2399.
- Moore, C. E. *Ionization Potentials and Ionization Limits Derived from the Analyses of Optical Spectra*; National Bureau of Standards: Washington, DC, 1970.
- Huber, K. P.; Herzberg, G. *Molecular Spectra and Molecular Structure. IV. Constants of Diatomic Molecules*; Van Nostrand Reinhold, Co.: New York, 1979, pp 99–116.
- <http://www.chemicool.com/elements/titanium.html>.
- (a) Helgaker, T.; Ruden, T. A.; Jorgensen, P.; Olsen, J.; Klopper, W. *J. Phys. Org. Chem.* **2004**, *17*, 913. (b) Min, S. K.; Lee, E. C.; Lee, H. M.; Kim, D. Y.; Kim, D.; Kim, K. S. *J. Comput. Chem.* **2008**, *29*, 1208. (c) Lee, E. C.; Kim, D.; Jurecka, P.; Tarakeswar, P.; Hobza, P.; Kim, K. S. *J. Phys. Chem. A* **2007**, *111*, 3446.
- Boese, A. D.; Oren, M.; Atasoylu, O.; Martin, L. M. L.; Kallay, M.; Gauss, J. *J. Chem. Phys.* **2004**, *120*, 4129.
- Zhao, Y.; Lusk, M. T.; Dillon, A. C.; Heben, M. J.; Zhang, S. B. *Nano Lett.* **2008**, *8*, 157.
- Wang, L.; Lee, K.; Sun, Y.-Y.; Lucking, M.; Chen, Z.; Zhao, J. J.; Zhang, S. B. *ACS Nano* **2009**, *3*, 3995.
- Yildirim, T.; Ciraci, S. *Phys. Rev. Lett.* **2005**, *94*, 175501.
- Durgun, E.; Ciraci, S.; Zhou, W.; Yildirim, T. *Phys. Rev. Lett.* **2006**, *97*, 226102.
- Zhang, C.-G.; Zhang, R.; Wang, Z.-X.; Zhou, Z.; Zhang, S. B.; Chen, Z. *Chem.—Eur. J.* **2009**, *15*, 5910.